A CRITIQUE OF STEAM HAMMER LOAD ANALYSIS METHODS

Trey W. Walters P.E.
Applied Flow Technology
Colorado Springs, Colorado, USA

PVP2022-83715

A CRITIQUE OF STEAM HAMMER LOAD ANALYSIS METHODS

Trey W. Walters, P. E.
Applied Flow Technology
Colorado Springs, Colorado, USA

ABSTRACT

One of the key assumptions in modern steam hammer load analysis is based on an incomplete understanding of steam wave behavior. Compression waves generated after a valve closure steepen much more quickly than previously thought. The resulting forces generated on pipe runs separated by elbows can be significantly higher than those predicted using current methods. To be more specific, current methods may give unconservative pipe force estimates – potentially resulting in unsafe designs. Using a more complete understanding of gas wave speed, quantitative examples are given which show the larger forces which occur as a result of wave steepening. Suggestions on how to improve load estimation are discussed.

KEYWORDS

Steam hammer, piping loads, transient simulation, transient compressible flow

NOMENCLATURE

Variables and symbols
a wave speed (ft/s / m/s)
A cross-sectional area (ft^2 / m^2)
c acoustic (sonic) velocity (ft/s / m/s)
D diameter (ft / m)
F force (lbf / kN)
K dimensionless pressure loss factor at pipe fitting
L length (ft / m)
L_C characteristic length (ft / m)
P static pressure (psi / kPa)
P_o stagnation pressure (psi / kPa)
T static temperature (F / C)
T_o stagnation temperature (F / C)
t time (sec)
t_c closing time of a valve (sec)
V fluid velocity (ft/s / m/s)

x axial distance (ft / m)
γ isentropic expansion coefficient
ρ static density (lbm/ft^3 / kg/m^3)
ρ_o stagnation density (lbm/ft^3 / kg/m^3)

Subscripts
b back (of wave)
f front (of wave)
J Joukowsky Eq.
M minus (direction in pipe)
SS steady-state

INTRODUCTION

One of the key unstated assumptions in modern steam hammer load analysis is that wave steepening is not significant in typical lengths of pipe runs. Recently Walters and Lang [1] conclusively showed that this assumption is mistaken.

For the last four decades the standard procedure for estimating steam hammer piping loads resulting from valve closures has been the Goodling Method [2-3]. There are several key assumptions made in the Goodling Method. One unstated assumption is that acoustic waves do not appreciably steepen.

Several papers have been published in recent years that used transient compressible flow numerical methods to evaluate wave steepening and the resultant generated forces. These papers used different numerical methods. Rovagnati and Gray [4-5] used an MOC (Method of Characteristics) tool, while Mayes, Gawande and Williams [6] and Mayes and Gawande [7] used a CFD tool. These four papers all observed wave steepening and larger forces than those given using Goodling or similar methods. However, no reasons for this behavior based on physics or theory were given by these authors.

Moody and Stakenborghs [8] recently discounted the claims in these papers and did so using physics and theory. However, Walters and Lang [1] showed that the reasoning in [8] had an oversight and neglected to consider how changes in bulk fluid

velocity of the gas affected wave speed. Walters and Lang developed analytical relationships to show why and how fast wave steepening occurs. They also used a commercially available software tool [9] to show the same wave steepening in a more real-world system which included friction and real gas effects. They showed that pipe forces can be much higher than Goodling predicts.

It will be shown in this paper what this means for steam hammer load analysis. Current methods of predicting forces are based on a mistaken assumption and are not conservative. Existing power station steam piping designed using the Goodling Method are not as safe as believed.

ACOUSTIC WAVE BEHAVIOR IN STEAM FLOW

When a valve closes in a steam line, a compression wave is generated upstream of the valve. This wave travels at a speed that depends on the bulk fluid velocity and the acoustic velocity of the steam. More generally, when a valve closes over some finite time, a family of compression waves is generated. The wave speed at the front of the wave family is not the same as the wave speed at the back of the wave family. This is due in part to a difference in acoustic velocities at the front and back (the back is at a higher temperature after the compression event and thus has a higher acoustic velocity) [8]. But, more importantly, the wave speed is different because the bulk steam velocity is different at the front and back of the wave family. This is discussed in detail using analytical relationships and diagrams by Walters and Lang [1].

It is well known that gas wave velocity, a, is a function of gas acoustic velocity, c, and gas bulk velocity, V:

$$a = V \pm c \qquad (1)$$

In that gas bulk velocity, V, is a vector, that makes gas wave velocity, a, also a vector. A compression wave like that discussed in this paper will follow Eq. 1 with the negative sign. A nomenclature distinction used here is that c represents gas acoustic velocity and a represents gas wave velocity. The terms gas *wave velocity* and gas *wave speed* are used interchangeably here with the understanding that both terms are vectors. Previous authors at times confused the concepts of gas acoustic velocity and gas wave velocity. This is part of the reason why wave steepening has been underestimated in the past.

Walters and Lang [1] gave an analytical relationship for the speed of wave steepening (the speed at which the back of the wave family catches the front) for a perfect gas in frictionless, adiabatic flow:

$$\Delta a_{fb} = \left| V_{SS}\left(\frac{\gamma+1}{2}\right) \right| \qquad (2)$$

where V_{SS} is the steady-state velocity and γ is the isentropic expansion coefficient. They showed that Eq. 2 is constant over time for frictionless, adiabatic flow of a perfect gas.

For adiabatic flow of real gases with friction the *initial* speed of wave steepening is given by:

$$\Delta a_{fb} = |c_b - c_{SS} + V_{SS}| \qquad (3)$$

where c_b is the sonic velocity at the back of the wave family and c_{SS} is the sonic velocity at the front (equal to the steady-state value). The bulk gas velocity at the front of the wave family is also the same as the steady-state gas velocity, V_{SS}. Eqs. 2 and 3 give the same result if the flow is frictionless and adiabatic and the gas is a perfect gas.

A quantitative example will be given which demonstrates the validity of Eq. 3 and also shows how the speed of wave steepening changes over time and distance from the initiating transient event. In other words, Eq. 3 is not constant in the flow of real gases with pipe friction.

ESTIMATING STEAM HAMMER LOADS USING GOODLING

Estimating steam hammer loads involves the rigorous application of Newton's Second Law of Motion. However, applying Newton's Second Law in steam hammer is complicated by the fact that transient compressible flow calculations are very difficult to obtain. If one does not have a reasonably accurate transient flow solution, then one cannot reliably use Newton's Second Law. This is for the simple reason that one does not know the necessary quantitative values in order to apply Newton.

Further, even if one was able to arrive at a trustworthy transient flow solution, one has to evaluate the importance of every term in Newton before deciding to start discarding terms in order to simplify. This will be discussed later in this section.

For now, let's look at the Goodling Method [2-3]. A maximum transient force is obtained using the Joukowsky equation pressure difference multiplied by the flow area and an uncertainty factor of 1.05:

$$F_{max} = \Delta P_J A * 1.05 \qquad (4)$$

The Joukowsky equation here uses the gas acoustic velocity and not the gas wave velocity. Eq. 4 is intended to predict the maximum possible transient force that occurs anywhere in the pipe assuming no diameter changes or reflections.

In addition, a "characteristic length" is determined from the following:

$$L_C = ct_c \qquad (5)$$

where t_c is closing time of the valve and c is the acoustic velocity as before.

Using Eqs. (4-5) one can determine the maximum force in a pipe leg (a run of pipe between direction changes – e.g., elbows) using the length of said pipe run:

$$F_{Leg} = F_{max}\frac{L_{Leg}}{L_C} \qquad (6)$$

If the length of the pipe run leg, L_{Leg}, is greater than the characteristic, L_C, then the force on the leg is simply equal to the

maximum force Eq. 4. The force profile shape typically looks like Fig. 1 for cases where $L_{Leg} < L_C$. For more on the Goodling Method force profile shapes, see [2-4].
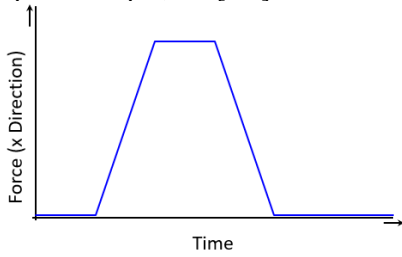

Figure 1. Typical transient force profile in pipe leg from a finite duration compression wave when $L_{Leg} < L_C$.

NUMERICAL SIMULATION OF STEAM HAMMER

The MOC has been a preferred method of simulating fluid transients in pipes for many decades. This is due in part to its unique advantages in simulating wave behavior. As noted earlier, References [4-5] used the MOC whereas [6-7] used CFD.

Using the MOC to simulate gas transients in general and steam hammer in particular is quite difficult. The fundamental equations are more complicated than for liquid flow (i.e., waterhammer/surge) and there are three equations (mass, momentum and energy) rather than two. As a result, two important accuracy issues emerge. First, the characteristic lines are markedly non-linear and there are three of them (as opposed to only two for liquid transients). Second, the characteristic lines do not lay nicely along a fixed grid. This means that one has to interpolate along grid points in the *x-t* plane. Both of these introduce significant uncertainties for the results.

There have been numerous MOC formulations in the literature. One particularly convenient formulation was published by Moody [10].

EXAMPLE 1

Rovagnati & Gray [4-5] appear to be the first to publish concerns about the Goodling Method. They used an in-house simulation tool which employed the Moody [10] formulation. Example 1 here is the same example used in [5] but here it will be explored in more depth. One difference here is that a different MOC tool is used which is of commercial quality [9] while still using the Moody formulation [10]. In principle, the results in [5] and [9] here should agree well. As you will see, in general they do agree but for several reasons (to be discussed) they are not in precise agreement. An advantage of [9] over [5] is that [9] has a generous feature set for reviewing and understanding the results – including animation capabilities which can be crucial in understanding pipe fluid transient results.

Example 1 Problem Statement

Note some of the problem statement data was not published in [5] but was included in the conference presentation – a copy of which was obtained from the authors of [5]. It was also confirmed that the presentation had a typo on pipe diameter.

There is a steam source at near-saturation conditions which flows through 1980 ft (604 m) of pipe to a turbine inlet. The

turbine inlet has a Turbine Stop Valve (TSV) which closes quickly to protect the turbine. All relevant data from [5] is listed below.

The in-house software tool used in [5] used a simplified steam properties table where the steam was treated as an ideal gas in some fashion. This was discovered after communication with the authors of [5]. The commercial tool used in this paper [9] allows one to use ASME Steam Table data which was used in all simulations presented in this paper. In addition to being more accurate, it also has saturation line data. Early simulation runs showed that the initial steady-state conditions fell below the saturation line in Example 1. This is important for an engineer using simulation tools because it can impact the accuracy of the calculation. Therefore, after some trial and error, the source condition temperature was slightly increased by 2 degrees F (~1 degrees C) such that all steady-state and transient results were superheated. With all the general uncertainty in engineering calculations, this minor change in temperature (and density) is negligible.

- Process conditions:
  - Assume all supply conditions are stagnation conditions (e.g., there is no velocity at these conditions – e.g., inside a vessel).
  - Steam source pressure
    - P_o = 1000 psia (6895 kPa)
  - Steam source non-pressures in Reference [5]
    - ρ_o = 2.24 lbm/ft^3 (35.9 kg/m^3)
    - T_o = 545 F (285 C)
  - Steam source non-pressures in Example 1 using Reference [9] (T_o increased by 2 deg. F to maintain superheated conditions)
    - ρ_o = 2.22 lbm/ft^3 (35.6 kg/m^3)
    - T_o = 547 F (286.1 C)
  - Initial flowrate
    - 1164 lbm/s (528 kg/s)
- Turbine Stop Valve (TSV)
  - Effective closure time t_c = 100 ms
  - Linear mass flowrate vs. time
- Single horizontal pipe run
  - Length = 1,980 ft (604 m)
  - Inner diameter = 29.25 inches (0.743 m)
  - Pipe roughness = 0.0018 in. (0.046 mm)
  - Adiabatic wall
  - Seven pipe legs of 40 ft. (12.2 m) length which are bounded by elbows pairs (Fig. 2.)
    - Legs 1, 4, 7, 10, 13, 16, and 19
  - All other legs are 125 ft (38.1 m) except for Leg 20 which is 200 ft (61 m)

Example 1 Goodling Method Results

As discussed at length in [5], the Goodling Method predicts the same maximum force and same force profile on all seven of the 40 ft (12.2 m) pipe run legs (depicted in Fig. 2).

To apply Eq. 4, one needs to calculate the pressure rise using Joukowsky at the TSV. To do that, one needs a reliable steady-

state solution at the TSV for an adiabatic pipe. A reliable solution can be obtained using various methods. Here we will use the steady-state results in [9] as shown in Table 1.
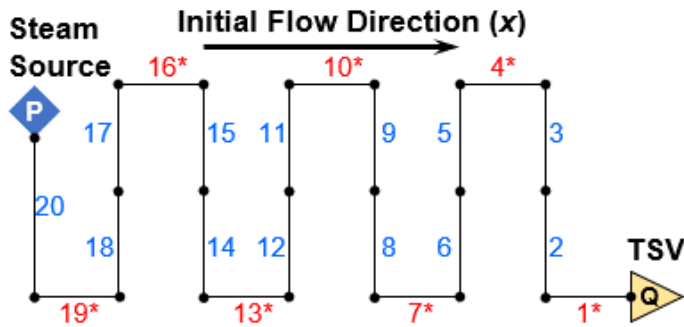

Figure 2. Schematic of Example 1 system with actual dimensions shown in the bullet list above for each pipe leg. Pipe legs with * symbol are those seven for which forces are calculated. Not to scale.

Table 1. TSV steady-state conditions at valve inlet (exit of pipe at Leg 1)

Parameter	Value at TSV
P_o	972.5 psia (6705 kPa)
P	969.4 psia (6684 kPa)
T	542.2 F (283.4 C)
ρ	2.157 lbm/ft^3 (34.6 kg/m^3)
V	115.6 ft/s (35.3 m/s)
c	1614 ft/s (492 m/s)
$a_M = V - c$	− 1498 ft/s (457 m/s)
γ	1.25

Using the values in Table 1 one can calculate the Goodling Method parameters. The Joukowsky equation is given by:

$$\Delta P_J = -\rho c \Delta V \qquad (7)$$

Since the TSV closes completely, the velocity goes from steady-state to zero. From Eq. 7 the pressure rise is a result of the velocity decrease. Hence ΔV is equal to -V. With these values and using Eqs. 4-7 we get the results in Table 2. Note that the F_{Leg} value applies to all seven of the 40 ft (12.2 m) pipe run legs.

Table 2. Example 1 results for Goodling Method

Parameter	Eq.	Calculated Result
ΔP_J	7	86.9 psid (599 kPa)
L_c	5	161.4 ft (49.2 m)
F_{max}	4	61,288 lbf (272.6 kN)
F_{Leg}	6	15,189 lbf (67.6 kN)

Example 1 Numerical Results (Min. 40 Pipe Sections)

Walters and Lang [1] established that the MOC method [9] gave results consistent with analytical results for an air system. Here [9] will be used on a steam system using ASME Steam Tables for steam properties and pipe friction.

As will be discussed in depth more later, numerical simulation results are affected by selection of the number of pipe computational sections as well as a few other numerical parameters. Here we will use computational sections and parameters consistent with those used in [5]. This was based on personal communication with the authors of [5] in which they used a minimum of 40 computational sections per pipe. In that the shortest pipe was 40 ft. (12.2 m) this means computational sections were 1 ft (0.3 m) long for all pipes.

Further, calculating transient forces from fluid transient simulation results is not as straightforward as one might think. Commonly, transient forces are estimated using just pressure differences along a pipe run leg. However, this simplification ignores other potentially significant contributors to the transient force balance. Lang and Walters [11] offer a detailed explanation of how to accurately calculate transient forces for liquid and gas transient systems. In short, the method is the same for liquids and gases as it is based on Newton's Second Law of Motion. However, different components of the force balance may be more important (or less) depending on whether the fluid is liquid or gas. It is not known exactly how [5] calculated forces from the simulation results but it is guessed that it was based on considering only the pressure terms in Newton and neglecting the others. Here forces will be shown based on a full accounting of all terms of Newton's Second Law [11]. Reference [9] incorporates everything in [11]. A comparison of forces calculated using [9 and 11] to the traditional $\Delta P*A$ approach will be given later.

Fig. 3 shows results for transient forces using 40 computational pipe sections. Table 3 shows the peak forces.

The Table 3 peak transient forces can be compared to that predicted by the Goodling Method in Table 2. The transient force in Leg 1 nearest the TSV is close to that predicted by Goodling in Table 2. However, it is clear that the transient forces in Table 3 Legs 4 and above are much higher than in Table 2.

Fig. 3 can be compared to results in Rovagnati and Gray's [5] Fig. 4. They show the forces with a negative sign so must be using a reverse x-direction coordinate system than used here. Regardless, Fig. 3 correlates well with that in [5] and in fact shows transient forces a bit higher by 15-20% than [5]. This could be for a number of reasons, including better accuracy using ASME Steam Tables and force calculation methods in [9]. The trend in Fig. 3 is also consistent with the more thoroughly explained analytical and numerical results in Walters and Lang [1]. However, further investigation will show that the story is even worse than shown in Fig. 3 when more computational sections are added. The use of a minimum of 40 computational sections per pipe was shown here to provide a better apples-to-apples comparison between this paper and [5]. Reference [5] did not evaluate sensitivity of predictions to pipe sectioning. Here we will.
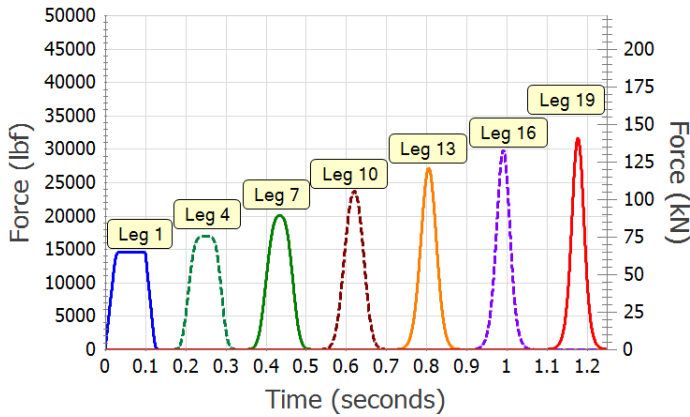
Figure 3. Transient force results on the pipe legs in the x direction for Example 1 system using minimum of 40 sections. Results obtained using [9].
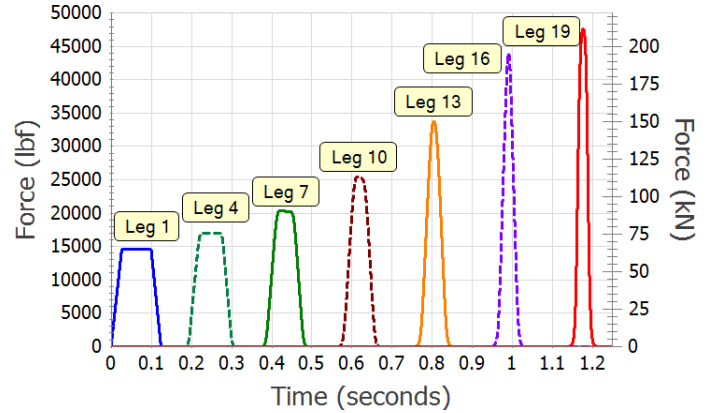

Figure 4. Transient force results on the pipe legs in the x direction for Example 1 system using minimum of 200 sections. Results obtained using [9].

Table 3. Peak forces from Fig. 3 (min. 40 pipe sections)

Leg #	Peak Force on Pipe Leg in x Direction		% Goodling
	lbf	kN	
1	14,609	65.0	96%
4	16,963	75.5	112%
7	20,133	89.6	133%
10	23,778	105.8	157%
13	27,190	121.0	179%
16	29,889	133.0	197%
19	31,721	141.2	209%

Table 4. Peak forces from Fig. 4 (min. 200 pipe sections)

Leg #	Peak Force on Pipe Leg in x Direction		% Goodling
	lbf	kN	
1	14,610	65.0	96%
4	16,985	75.6	112%
7	20,361	90.6	134%
10	25,469	113.3	168%
13	33,823	150.5	223%
16	44,019	195.9	290%
19	47,699	212.2	314%

Example 1 Numerical Results (Min. 200 Pipe Sections)

Two changes are made for this simulation compared to the previous to obtain better accuracy than in Fig. 3. The first is that a finer grid is used with a minimum of 200 sections per pipe. In that the shortest pipe is 40 ft. (12.2 m) this means computational sections are 0.2 ft (2.4 in., 6.1 cm) long for all pipes.

The second simulation change is an artifact of using MOC for transient compressible flow. The Appendix provides a brief explanation. In summary, a grid and time step as shown in Fig. A-2 will be used here. The Fig. A-1 grid was used in obtaining the Fig. 3 results.

The results are shown in Fig. 4. Table 4 summarizes the peak transient pressures. While Table 3 shows a peak transient force over twice that of the Goodling Method, Table 4 shows it as over three times as high!

Clearly, comparing results from Figs. 3 and 4 show that there is substantial sensitivity of peak transient forces to computational sections used. Maybe using more than a minimum of 200 sections will yield even higher forces? Fig. 5 shows the sensitivity of peak transient forces using 5-200 pipe computational sections in each pipe at minimum. All cases in Fig. 5 use a grid like that in Fig. A-2.

What can be learned from Fig. 5? It appears that the peak forces level out for pipe Legs 1, 4, 7 and 10. But pipe Legs 13, 16 and 19 are still rising slightly. Hence, looking at Table 4, the peak forces are reliable for the first four legs. The final three may not be a true peak. Another corollary thing we learned is that users of numerical simulation tools for steam hammer using the MOC should be extra careful to make sure they are using a sufficient number of pipe of sections such that they are capturing a true maximum. For those not familiar with MOC methods, this is easier said than done. There is an exponential squared relationship for number of sections and computer run time. In other words, a run time for the 200-section case takes $(200/40)^2$ = 25 times longer than the 40-section case.

What does this have to do with the wave steepening effect discussed earlier? It has everything to do with it. Let's explore this further.

Fig. 6 shows the path of the front and back of the wave family for the 200-section simulation. Three insightful things can be learned from Fig. 6.
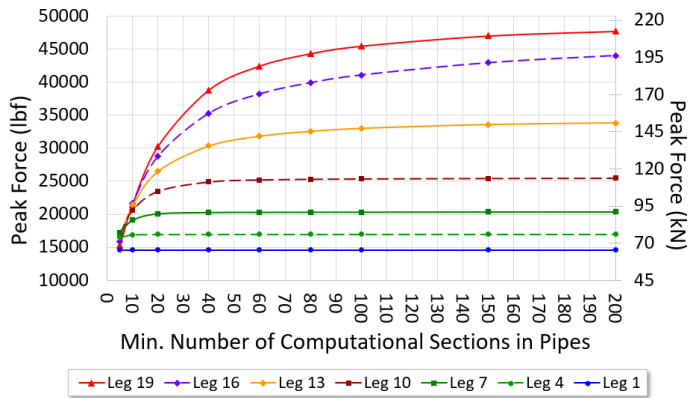
Figure 5. Peak transient forces for a range of computational pipe sections. Results obtained using [9].
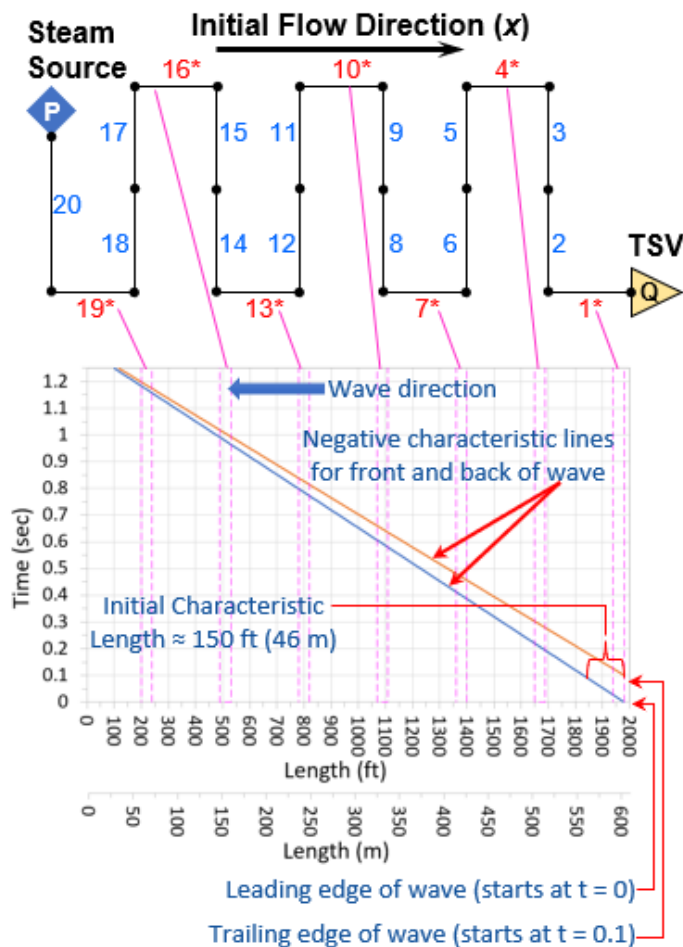

Figure 6. Positive and negative characteristic lines follow the front and back of the wave family for 200-sections case.

First, it is clear in Fig. 6 that the back of the wave (which starts at 0.1 seconds) is catching up with the front (which starts at 0 seconds). This means that the wave family is steepening.

Second, the initial characteristic length (L_c) is about 150 ft (46 m). This is hard to see in the small size of Fig. 6 but can be

clearly seen in a larger graph. This length is shorter than the Goodling Method predicts in Table 2. Why? This will be answered shortly.

Third, the characteristic length (if there even is one) changes with time. More on this below.

On the second item above, a clue is given in Table 1. The steam wave speed, a_M, is shown there as 1,498 ft/s (457 m/s). The negative sign is because the steam compression wave is moving from right to left in Fig. 6.

If one uses a_M in Eq. 5 rather than c one obtains:

$$L_C = a_M t_c \qquad (8)$$

which obtains a value of 150 ft (46 m). This is consistent with results in Fig. 6 for characteristic length.

A moment's thought about the concept of characteristic length leads to an obvious conclusion. The characteristic length is attempting to capture how far a wave moves over some time Δt. The wave does not move at the acoustic velocity, c. It moves at the *wave* velocity, $V - c$, which is a_M. In other words, Eq. 5 is not correct. Those wishing to use the Goodling Method should use Eq. 8 to calculate the characteristic length.

As Fig. 6 has the wave family front and back *positions* with time, it is a simple matter to plot the wave *speed* of the front and back of the wave family. This is shown in Fig. 7. Here one can see that, for real gas simulations with friction, the front and back wave speeds are not constant with time.
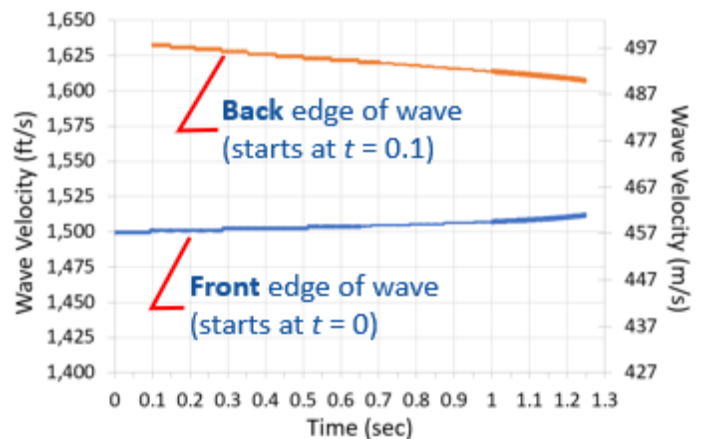

Figure 7. Wave velocity at front and back of wave family for 200-sections case.

Also of interest in Fig. 7 is the difference in velocities of the two curves when the TSV closes at 0.1 seconds. The top curve for the back of the wave family is roughly 1,633 ft/s (498 m/s). The bottom curve for the front of the wave family at 0.1 sec is 1,499 ft/s (457 m/s). Again, these are *wave velocities*, a, and *not* acoustic velocities, c.

Subtracting these two values gives the speed at which the back of the wave is catching up with the front, Δa_{fb}. This comes out to about 134 ft/s (41 m/s).

6

Now we can look back to Eq. 3. We take the values in Table 1 for V_{SS} and c_{SS} but we need to know c_b. We can estimate the pressure at the TSV at $t = 0.1$ by using the Joukowsky Equation pressure rise (Table 2) and the initial pressure in Table 1. This obtains a static pressure of about 1,056 psia (7,281 kPa). Taking the pressure rise as isentropic (as a rough estimate as it really isn't isentropic because there is friction involved) obtains a temperature at 0.1 seconds of 560 F (293 C). From there a value of c_b can be obtained from steam tables of 1,628 ft/s (496 m/s). The value from Eq. 3 Δa_{fb} is roughly 130 ft/s (40 m/s) which agrees fairly well with the Fig. 7 estimate above of 134 ft/s (41 m/s). Realize this is imperfect because the Joukowsky Equation pressure rise is for an instant valve closure while the valve in Example 1 closes over 0.1 seconds. For good measure, use of Eq. 2 (developed for a perfect gas behavior in frictionless flow [1] so not 100% applicable to our case either) also gets a value of 130 ft/s (40 m/s) using Table 1 values as input.

Putting this all together, the back of the wave is initially catching up with the front at about 134 ft/s (41 m/s). Over time, the difference between the front and back wave speeds (Fig. 7) decreases. This means effectively that Δa_{fb} decreases over time.

Using results from Figs. 6 and 7 one can determine how the characteristic length changes over time – see Fig. 8. This is another way of saying that the concept of "characteristic length" itself is flawed. There is no characteristic length. There is an *initial* characteristic length given by Eq. 8 (*not* Eq. 5). But as time goes on and the wave family moves further from the source, the so-called characteristic length shrinks. This happens because the back of the wave catches up with the front (Fig. 6) as the wave steepens.

As noted earlier, Eq. 8 predicts an initial characteristic length of 150 ft (46 m) which is confirmed by Fig. 8 at 0.1 seconds.
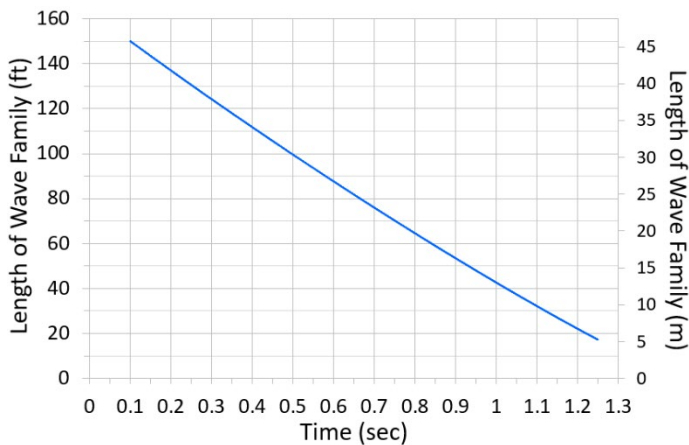

Figure 8. The length of the wave family (usually called the characteristic length) for 200-sections case.

One can clearly see the wave steepening by looking at time snapshots of the pressure profile. The top graph in Fig. 9 shows the shape of the pressure profile in a sequence of time slices as the wave moves from right to left. It is clear that the wave

steepens. For example, at $t = 0.1$ seconds, right after the TSV closed, the pressure wave does not come close to fitting inside the 40 ft (12.2 m) pipe Leg 1. As the wave moves to the left, each time slice has more of the wave fit inside the pipe leg at that location. Finally, when the wave reaches Leg 19 the entire wave fits inside the leg. This creates the maximum force as shown in Fig. 4.

Also shown in Fig. 9 for interest are the corresponding fluid velocity, V, profiles and acoustic velocity, c, profiles.
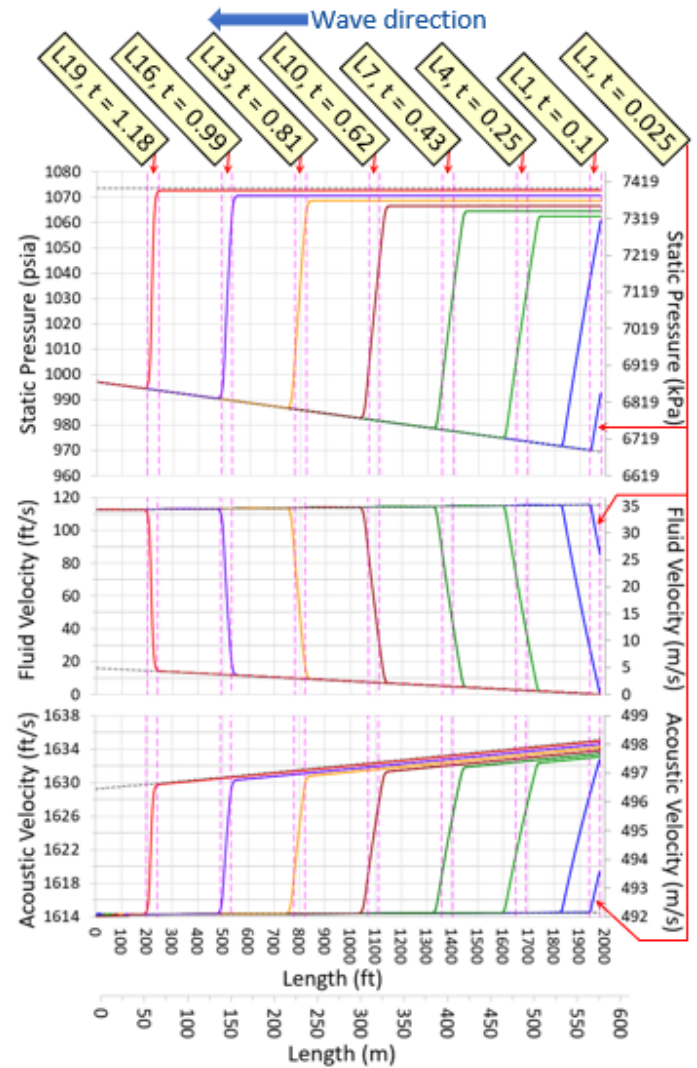

Figure 9. Profiles at various times for static pressure, fluid velocity and acoustic velocity for 200-sections case. Wave moves to the left so each profile from right to left is at a later time (shown at top in seconds). Physical locations for pipe Legs 1, 4, 7, 10, 13, 16 and 19 shown as dashed vertical lines.

MORE ON CALCULATING FORCES

As discussed earlier, Lang and Walters [11] discuss how to calculate transient forces using all terms in Newton's Second Law. There is a traditional approach to calculating transient forces whereby only the Pressure x Area terms are used in Newton – neglecting all other terms. There are situations where

the traditional method is acceptably accurate, and there are situations where it is highly inaccurate. These are discussed in [11].

With pressure profiles available such as shown in Fig. 9, one can use the traditional approach and compare that to a full force balance. Table 5 shows this comparison. Here, one can see that, at least for Example 1, the traditional approach predicts higher forces than the complete approach by about 10%.

Table 5. Forces for 200-sections case using ΔP method and the complete force balance method in [9, 11].

Leg #	Max ΔP (psid / kPa)	Peak Force Using $\Delta P*A$ (lbf / kN)	Peak Force Using All Terms [9, 11] (lbf / kN)
1	24.2 / 167	16250 / 72	14610 / 65
4	27.9 / 192	18758 / 83	16985 / 76
7	33.3 / 229	22351 / 99	20361 / 91
10	41.3 / 285	27750 / 123	25469 / 113
13	54.3 / 374	36491 / 162	33823 / 151
16	70.6 / 487	47435 / 211	44019 / 196
19	76.6 / 528	51451 / 229	47699 / 212

EXAMPLE 2

This example has all the same conditions as Example 1, except it attempts to assess the importance of pressure losses at the elbow pairs.

A K factor of 0.168 was used at all elbows. The steady-state pressure loss of each was roughly 0.5 psid (3.5 kPa). In that there were 13 elbows in this model, this added roughly 6.7 psid (46.4 kPa) pressure drop.

As the flowrate is constrained at 1,164 lbm/s (528 kg/s), the conditions at the pipe exit to the TSV (the TSV inlet) will be impacted. The equivalent values in Table 1 will be different – not dramatically different, but different. For example, Example 1 has a steady-state pressure drop in the pipes of about 28 psid (190 kPa). Hence the elbows increase the pressure loss by about 20%.

The purpose here is not to provide all the same details given in Example 1. Rather, it is just to show the trends in transient force predictions when one accounts for elbow losses.

Obviously, this is well beyond the reach of analytical solutions. The Reference [9] tool can include losses at fittings and components. It assumes the steady-state K factors remain the same during the transient simulation. As before, this simulation uses 200 computational sections and the grid time-step scheme in Fig. A-2. Fig. 10 shows the transient forces for this case while Table 6 summarizes the peak forces.

Comparing Table 6 to Table 4 shows little impact on the pipe legs closest to the TSV. The legs farthest away (16 and 19) have forces 4% lower.
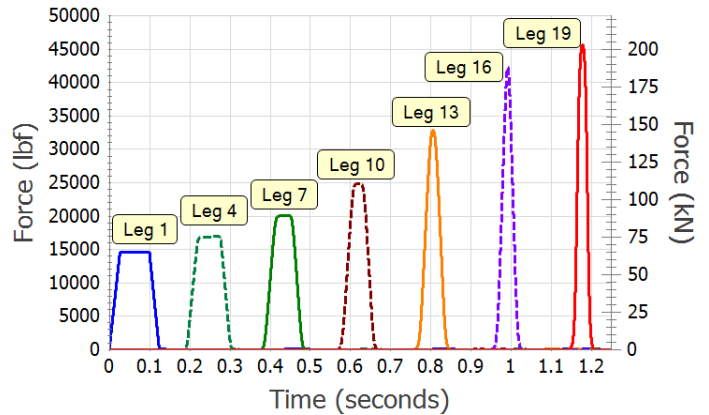

Figure 10. Transient force results on the pipe legs in the x direction for Example 2 system using minimum of 200 sections.

Table 6. Peak forces from Fig. 10 with losses at elbows.

Leg #	Peak Force on Pipe Leg in x Direction		% Goodling
	lbf	kN	
1	14,635	65.1	96%
4	16,954	75.4	112%
7	20,144	89.6	133%
10	24,913	110.9	164%
13	32,880	146.3	216%
16	42,350	188.4	279%
19	45,706	203.4	301%

EXAMPLE 3

One final example is offered here. All input conditions are the same as Example 1, except the flowrate is at a 20% uprated value of 1,397 lbm/s (634 kg/s). Similar to Example 2, this will impact conditions at the exit of the pipe and inlet to the TSV with extra pressure drop. Again, the purpose here is to show a trend and not every detail of the example input and output.

Fig. 11 shows the transient forces. An item of interest is the trend of increasing force with length (e.g., Fig. 4) is different in Fig. 11. Here one can see how the peak transient forces in pipe Leg 19 are lower than in pipe Leg 16. Walters and Lang [1] discuss this possibility. It is caused by two competing effects. The first effect is the increased wave steepening the further one is from the source of the transient. This is discussed at length in the present paper.

The second effect is reduced potential driving pressure because the steady-state pressure drop is lower the farther from the transient source. This means a narrower "envelope" of driving pressure.
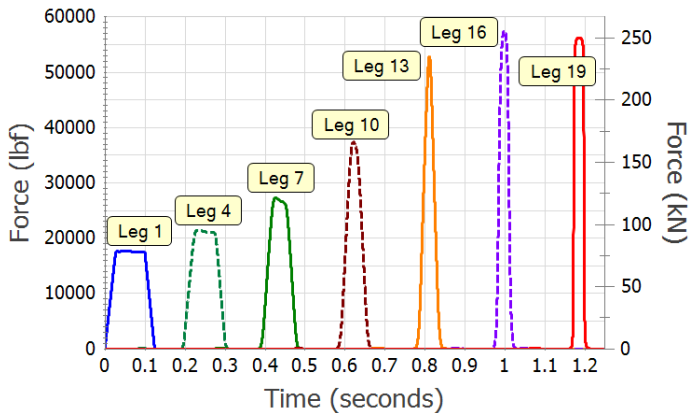
Figure 11. Transient force results on the pipe legs in the x direction for Example 3 system using minimum of 200 sections. Note maximum y-axis scale is larger than for previous figures.

DISCUSSION

The examples presented in this paper clearly show that the Goodling Method does not reliably yield conservative pipe loads. This confirms earlier reports and especially those in [5]. The examples here show that a more detailed model than used in [5] produces transient forces much higher than reported in [5]. Combined with the theoretical and physics-based explanation in [1], there are well-founded reasons to mistrust the Goodling Method.

The examples presented here show that the missing piece which the Goodling Method does not account for is wave steepening. The wave steepening effect has been shown with analytical solutions in [1] and also shown numerically for steam flow (in this paper) and for air flow [1].

Including the effect of elbow losses reduces peak forces a relatively small amount (0-4%) between the Example 1 and 2 systems.

Numerical simulation results are sensitive to the number of computational sections used (Fig. 5) and to the grid scheme (see Appendix). Future analysts applying MOC to steam hammer should take great care in these modeling choices. Indeed, Fig. 5 suggests that the peak forces for the legs farthest from the TSV have still not reached a true maximum. Additional safety factors should thus be applied to these forces and/or additional simulation runs should be made with even more computational sections.

Alarmingly, the findings presented here call into question all pipe structural analyses past and present that have relied on the Goodling Method – or any similar method which neglects wave steepening. As one can find the Goodling Method being used on nuclear power station piping [12], the findings here call into question the safety of all such piping systems.

RECOMMENDATIONS

1. Existing systems designed using the Goodling Method should be re-evaluated for maximum pipe loads for safety reasons. Strengthened pipe supports should be added where deemed necessary.
2. Going forward, engineers should consider using a capable simulation tool to determine peak loads and load profiles.
3. Engineers should not trust the Goodling Method or any similar method which neglects wave steepening. A new alternative to the Goodling Method which incorporates wave steepening effects is given by Walters [13].

CONCLUSIONS

Traditional methods for evaluating transient piping loads (such as the Goodling Method [2-3]) do not reliably give conservative pipe loads. Wave steepening is not accounted for in such methods. Systems designed using the Goodling Method are likely not as safe as previously believed. This includes nuclear power station piping in recent decades.

The Goodling Method should not be used for steam piping load estimation except perhaps in very short pipe runs. Engineers should seek other methods that can yield more accurate estimates.

REFERENCES

[1] Walters, T.W. and Lang, S.A. (2022), "How fast is a finite gas transient wave and why does it steepen?", Proc. 14th International conference on pressure surges, BHR Group, Prague, Czech Republic, November 2022 (note this conference was recently delayed from April to November 2022 due to COVID-19).

[2] Lee, M. Z., and Goodling, E. C., (1982), "Steamhammer in Power Plant Piping Restraint Design and Optimization", ASME Pressure Vessels and Piping Conference, Orlando, Florida, USA, Vol. 69, June 27, 1982.

[3] Goodling, E. C., (1989), "Simplified Analysis of Steam Hammer Pipe Support Loads", ASME/JSME Pressure Vessels and Piping Conference, Honolulu, Hawaii, USA, July 23-27, 1989, PVP Vol 165.

[4] Rovagnati, B, and Gray, J. H., (2014), "Effect of Reflection Waves on Water Hammer Loads", ASME Pressure Vessels & Piping Conference, Anaheim, California, USA, July 20-24, 2014, PVP2014-29121.

[5] Rovagnati, B, and Gray, J. H., (2015), "Fluid Compressibility Effects In Steam Hammer Analyses", ASME Pressure Vessels & Piping Conference, Boston, Massachusetts, USA, July 19-23, 2015, PVP2014-29121.

[6] Mayes, A., Gawande, K. P. and Williams, D. K., (2017), "Comparisons of CFD and Traditional Solutions For Steam Hammer Events", ASME Pressure Vessels & Piping Conference, Waikoloa, Hawaii, USA, July 16-20, 2017, PVP2017-65864.

[7] Mayes, A. and Gawande, K. P., (2018), "Effect Of Steam Hammer Pressure Wave Steepening On Pipe Supports", ASME Pressure Vessels & Piping Conference, Prague, Czech Republic, July 15-20, 2018, PVP2018-84775.

[8] Moody, F. J., and Stakenborghs, R., (2018), "The Effects Of Compressibility And Piping Geometry On Steamhammer Loads", 26th International Conference on Nuclear

Engineering, London, England, July 22-26, 2018, ICONE17-75743.

[9] Applied Flow Technology, (2022), *AFT xStream* software tool, Colorado Springs, CO, USA.

[10] Moody, F. J., (1990), Introduction To Unsteady Thermofluid Mechanics, Wiley-Interscience, 1990.

[11] Lang, S.A. and Walters, T.W. (2022), "Accurately Predicting Transient Fluid Forces in Piping Systems – Part 1: Fundamentals and Part 2: Applications", ASME Pressure Vessels & Piping Conference, Las Vegas, NV, USA, July 17-22, 2022, PVP2022- 84740 and -84748

[12] Stakenborghs, R., and Dziuba, L., (2009), "Simplified Approach to Establishing Bounding Main Steam Piping Support Load Increase Due to Reactor Power Uprate", 26th International Conference on Nuclear Engineering, Brussels, Belgium, July 12-16, 2009, ICONE17-75743.

[13] Walters, T.W. (2022), "Improved Method of Estimating Steam Hammer Loads", ASME Pressure Vessels & Piping Conference, Las Vegas, NV, USA, July 17-22, 2022, PVP2022-83717.

APPENDIX

There is a grid selection numerical artifact when using the MOC for transient compressible flow [9-10]. The details on this are frankly beyond the scope of this paper. A brief explanation will be given here but interested readers should consult [9-10] for a more in-depth explanation.

Because interpolations are required between grid points, stability is ensured by choosing a Δx (pipe section length) and Δt (time step) that captures all possible wave position changes. This happens at $2*c_{max}$. Here c_{max} is the maximum acoustic velocity at any location and time during the entire simulation. This is almost always the acoustic velocity at the maximum gas temperature. See Fig. A-1.

However, if one knows the maximum Mach number during the simulation, a different grid can be used which essentially uses a longer time step. This offers a double benefit – enhanced accuracy and shorter run times (because of the longer time step).

The Example 1 system has a maximum Mach number of about 0.08 which would suggest using $1.08*c_{max}$. Hence, a grid like that in Fig. A-2 which uses $1.1*c_{max}$ can be safely used.

The MOC grid is depicted in Figs. A-1 and A-2 where R, L and P represent, respectively, the characteristic lines for Right, Left and Particle Path. The numbers represent grid point locations.
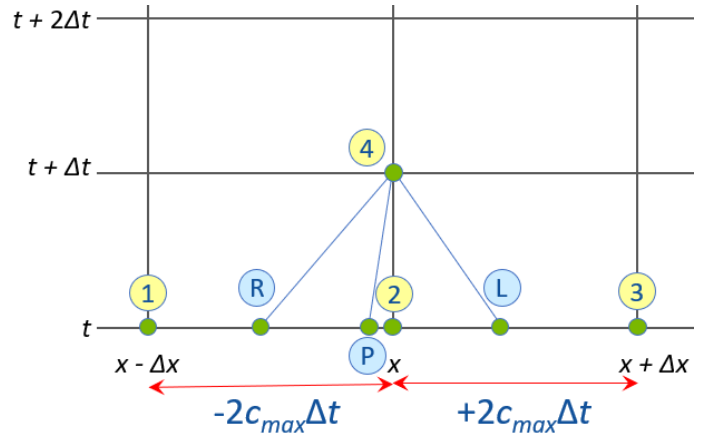

Figure A-1. Standard grid using $\Delta x = +/- 2c_{max}\Delta t$ is always stable.
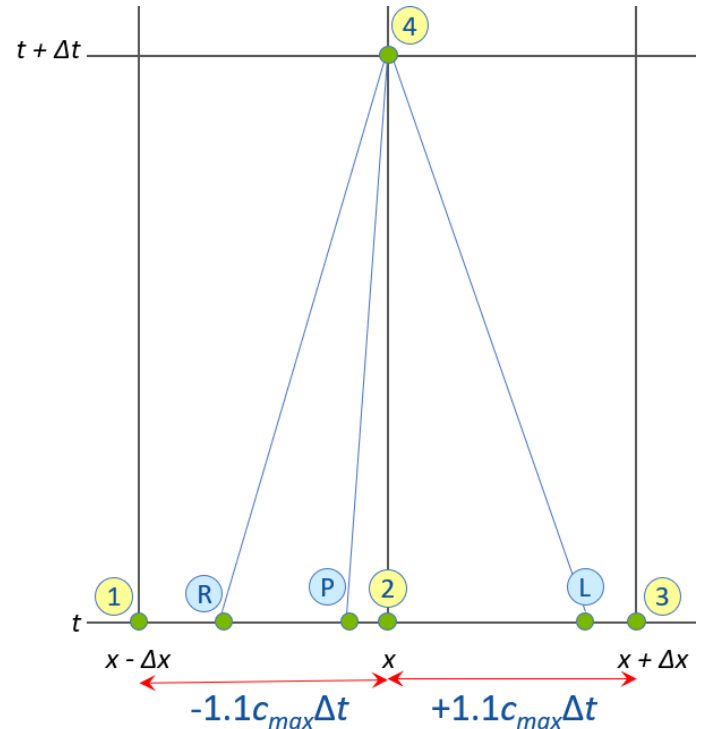

Figure A-2. Enhanced grid using $\Delta x = +/- 1.1c_{max}\Delta t$ can be used with knowledge of the maximum Mach number. The time step here is longer than in Fig. A-1.